International Journal of Mathematical, Engineering and Management Sciences
Vol. 8, No. 5, 927-942, 2023
https://doi.org/10.33889/IJMEMS.2023.8.5.053

Modeling Developable Surfaces using Quintic Bézier and Hermite Curves

Kusno
Department of Mathematics,
University of Jember, Jember, Indonesia.
E-mail: kusno.fmipa@unej.ac.id

(Received on March 3, 2023; Accepted on June 14, 2023)

Abstract
The nature of the developable surfaces has similarities to the industrial materials that are not amenable to stretching. Regarding the benefit, the developable surfaces are widely used to model plat-metal-based industry products such as automobiles, ship hulls, and ducts. For this reason, we introduce a new approach for designing developable surfaces limited by two space curves. The method consists of these steps. First, we define a generalized cone and a cylinder surface by posing restrictions: a fixed summit point of the cone has to be outside a plane; a static nonzero constant vector is unparallel to the plane; and two quintic Bézier curves are placed on the different sides of the plane. Second, computing the control points on the plane is determined by the intersection between the control lines of the cone/cylinder surface and the plane. Third, using these obtained control points, we evaluate the required boundary curves profile and the shape of the developable Bézier surfaces, that are limited by these quintic Bézier curves. Finally, we also apply this method to design the developable Hermite surfaces. As a result, this introduced method can provide the equations and procedures for modeling developable surfaces with boundary curves in space. Also, it is useable to design these surfaces in many arches and shapes. Moreover, this method is effective for modifying and adjusting the desired boundary curves profile of the surfaces.

Keywords- Boundary curves, Developable surfaces, Generalized cone/cylinder surfaces, Quintic Bézier/Hermite curves.

1. Introduction

Mathematical studies addressing the developable surface construction have been introduced. Park et al. (2002) presented the surfaces using a set of rulings and calculations of the existence of directrix curves to obtain the developable surfaces. In the context of constructing the directrix curves, they determined a class of objective functions. Then, Zhao and Wang (2008) introduced a method to define the developable surface by employing the surface pencil passing a given curve. From a geodesic curve of a developable surface, Al-Ghefari and Abdel-Baky (2013) evaluated a method for designing a tangent lines surface, cylinder, and cone surface.

Xu et al. (2017) studied the developable surface of IGA-suitable planar B-spline parameterizations using complex CAD boundaries. However, constructing the surface needs many operations. Hu et al. (2018) reported the formulation of generalized developable H-Bézier surfaces by employing control planes through generalized H-Bézier basis functions. Then, Abdel-Baky and Unluturk (2020a) constructed a developable tangent surface to a surface along a curve on the surface. They also examined a normal developable surface of a surface along a normal direction curve (Abdel-Baky and Unluturk, 2020b).

Concerning the industrial application approach, Frey and Bindschadler (1993) designed the developable Bézier patches using the restriction that the tangent vectors of their boundary curve must be parallel. The technique is generally easy to use for creating developable surfaces. Unfortunately, calculating equations system of the Bézier control points is still not stable and deterministic. Besides that, the boundary curves are plane curves. Kusno (2019) developed Frey and Bindschadler's work by utilizing the boundary curves of the surfaces at four, five, and six degrees in a plane, respectively, and employing a deterministic calculation method. Then, using the tangent vector criteria of these boundary curves, he presented the construction of developable Hermite patches (Kusno, 2020b; Kusno, 2021).

Fernández-Jambrina and Pérez-Arribas (2020) studied the developable patches designed through NURBS curves. Then, utilizing a dual method, Li and Zhu (2020) modeled C-Bézier developable surfaces with some parameters. Ammad et al. (2021) recently introduced a new way to construct developable cubic trigonometric Bézier surfaces. This method provides some shape control parameters for designing the two boundary curves profile of the surfaces. However, these parameters can change only one of the two boundary curves shape dominantly.

The presented methods generally have some limitations. The introduced equations cannot be implemented efficiently for designing the surfaces, and the boundary curves must be laid in the planes. The control parameters of these equations can modify the curve shape, but it happens only in one boundary curve. In consequence, we need a new method for constructing the surfaces to avoid these restrictions.

This article presents a new approach for designing developable surfaces limited by quintic Bézier and Hermite curves in space. Moreover, we numerically test and simulate the shapes of these surfaces.

2. Quintic Developable Bézier Surfaces Construction

In this section, we organize the discussion in some stages. The first stage discusses the mathematical theory for defining developable surfaces and the quintic Bézier curve. In the second step, we introduce the numerical approach for designing quintic developable Bézier surfaces of generalized cone surfaces. Finally, we present the quintic developable Bézier surfaces of cylinder surface. The modeling results of these surfaces are simulated using a mathematical tool.

There are three types of surfaces locally isometric to a plane called developable surfaces, i.e., generalized cone, cylinder, and tangent surface. Their tangent planes are constant for all points of a generator line of the surfaces (Lipschutz, 1969; Julius, 2006; Yu, 2017). These surfaces can be developed (unfolded) onto the plane. Meanwhile, their shapes can be designed from a planar surface without tearing or stretching. Due to the surfaces being similar to the materials that are not amenable to stretching, they are widely used to model the plat-metal-based industries, i.e., automobiles, ships, clothing, shoes, and ducts. For this reason, we design the developable Bézier and Hermite surfaces bounded with the space curves using definitions of generalized cone and cylinder surfaces in the algebraic equations, respectively (Abbena et al., 2006; Julius, 2006; Yu, 2017).

$$\mathbf{S}(u,v) = \mathbf{O} + v\,\mathbf{G}(u) \tag{1}$$

$$\mathbf{S}(u,v) = \mathbf{G}(u) + v\,\mathbf{U} \tag{2}$$

where, $\mathbf{O}\in\mathbf{R}^3$ is a fixed nonzero constant vector as the summit point of the cone surface, the curve $\mathbf{G}(u)$ is the directrix or based curve, and the fixed nonzero direction vector $\mathbf{U}\in\mathbf{R}^3$ is the generatrix of the cylinder surface. In order to the plat-metal-based industries application, we determine the curve $\mathbf{G}(u)$ in Equation (1) in the form $\mathbf{G}(u) = [\mathbf{P}(u) - \mathbf{O}]$. Therefore, Equation (1) can be expressed in the linear combination of the vector $\mathbf{O}$ and the curve $\mathbf{P}(u)$ as follows:

$$\mathbf{S}(u,v) = \mathbf{O} + v\,[\mathbf{P}(u) - \mathbf{O}] = (1\text{-}v)\,\mathbf{O} + v\,\mathbf{P}(u) \tag{3}$$

On the other hand, the regular Bézier curve of degree n is defined in the form,

$$\mathbf{P}(u) = \sum_{i=0}^{n} \mathbf{P}_i \, B_i^n(u).$$

where, $B_i^n(u) = C_i^n.(1-u)^{n-i}.u^i$; $C_i^n = \frac{n!}{i!\,(n-i)!}$ and $0 \le u \le 1$. When $n = 5$, it becomes a quintic Bézier as given by Equation (4),

$$\mathbf{P}(u) = \mathbf{P}_0\,(1-u)^5 + 5\mathbf{P}_1\,(1-u)^4\,u + 10\mathbf{P}_2\,(1-u)^3\,u^2 + 10\,\mathbf{P}_3\,(1-u)^2\,u^3 + 5\mathbf{P}_4\,(1-u)\,u^4 + \mathbf{P}_5\,u^5 \quad (4)$$

where, $\mathbf{P}_0$, $\mathbf{P}_1$, $\mathbf{P}_2$, $\mathbf{P}_3$, $\mathbf{P}_4$, and $\mathbf{P}_5$ are the control points of the curve $\mathbf{P}(u)$. The term of the control point $\mathbf{P}_0$ expresses a point P_0 with the position vector $\mathbf{P}_0 = <x_0, y_0, z_0>$. A notation with a bold letter means a vector value, and the italic alphabets x_0, y_0, and z_0 express the real numbers.

2.1 Quintic Developable Bézier Surfaces Defined with Generalized Cone Surface

Consider a generalized cone surface $\mathbf{S}_1(u,v) = \mathbf{O} + v\,[\mathbf{P}(u) - \mathbf{O}]$ and the curve $\mathbf{P}(u)$ of the regular quintic Bézier curve of Equation (4). We restrict that the curve $\mathbf{P}(u)$ is laid between the fixed point $\mathbf{O}$ and a plane $\mathbf{\Psi}(t,w) = \mathbf{n} + t\,\mathbf{b} + w\,\mathbf{c}$. In addition, the direction of the curve $\mathbf{P}(u)$ and the plane $\mathbf{\Psi}(t,w)$ are in the same orientation such that, for every point of position vector $\mathbf{P}(a)$ on the curve $\mathbf{P}(u)$ with the value a in the interval $0 \le a \le 1$, the extension of a line $\mathbf{O} + v\,[\mathbf{P}(a) - \mathbf{O}]$ intersects at a unique point $\mathbf{Q}(v)$ in the plane $\mathbf{\Psi}(t,w)$ as follows (Mortenson, 1986),

$$\mathbf{Q}(v) = \mathbf{O} + v\,[\mathbf{P}(a) - \mathbf{O}] = \mathbf{n} + t\,\mathbf{b} + w\,\mathbf{c} \quad (5)$$

By employing vector and scalar products, we can calculate,

$$v = \frac{(\mathbf{b}\wedge\mathbf{c}).(\mathbf{n}-\mathbf{O})}{(\mathbf{b}\wedge\mathbf{c}).[\mathbf{P}(a)-\mathbf{O}]} \quad (6)$$

Consequently, the intersection points $\mathbf{Q}(u)$ in the plane $\mathbf{\Psi}$ are,

$$\mathbf{Q}(u) = \mathbf{O} + \left[\frac{(\mathbf{b}\wedge\mathbf{c}).(\mathbf{n}-\mathbf{O})}{(\mathbf{b}\wedge\mathbf{c}).[\mathbf{P}(u)-\mathbf{O}]}\right][\mathbf{P}(u) - \mathbf{O}] = \mathbf{O} + \alpha(u)\,[\mathbf{P}(u) - \mathbf{O}] \quad (7)$$

where, $\alpha(u)$ is a real function (scalar) with $\alpha(u) > 1$.

In conclusion, if the control points $[\mathbf{P}_0,\mathbf{P}_1,\mathbf{P}_2,\mathbf{P}_3,\mathbf{P}_4,\mathbf{P}_5]$ define the quintic Bézier curve $\mathbf{P}(u)$ in space, then, for $i = 0, 1,\ldots,5$, prolonging lines $\mathbf{O} + v\,[\mathbf{P}_i - \mathbf{O}]$ from the summit point $\mathbf{O}$ to the plane $\mathbf{\Psi}$ gets the intersection control points $[\mathbf{Q}_0,\mathbf{Q}_1,\mathbf{Q}_2,\mathbf{Q}_3,\mathbf{Q}_4,\mathbf{Q}_5]$ in the plane $\mathbf{\Psi}$. We can state,

$$\mathbf{Q}_i = \mathbf{O} + \left[\frac{(\mathbf{b}\wedge\mathbf{c}).(\mathbf{n}-\mathbf{O})}{(\mathbf{b}\wedge\mathbf{c}).[\mathbf{P}_i-\mathbf{O}]}\right][\mathbf{P}_i - \mathbf{O}] = \mathbf{O} + \alpha_i\,[\mathbf{P}_i - \mathbf{O}] \quad (8)$$

where, the real scalars $\alpha_i > 1$.

On the contrary, because for $0 \le u \le 1$, the lines $\mathbf{O} + \alpha(u)\,[\mathbf{P}(u) - \mathbf{O}]$ intersect 1-1 to the plane $\mathbf{\Psi}$, and the control points $[\mathbf{P}_0,\mathbf{P}_1,\mathbf{P}_2,\mathbf{P}_3,\mathbf{P}_4,\mathbf{P}_5]$ determine $[\mathbf{Q}_0,\mathbf{Q}_1,\mathbf{Q}_2,\mathbf{Q}_3,\mathbf{Q}_4,\mathbf{Q}_5]$ on the plane $\mathbf{\Psi}$, using these control points $\mathbf{Q}_i$ for $i = 0, 1,\ldots,5$ get $[\mathbf{P}_0,\mathbf{P}_1,\mathbf{P}_2,\mathbf{P}_3,\mathbf{P}_4,\mathbf{P}_5]$ that construct the space curve $\mathbf{P}(u)$ as follows:

$$\mathbf{P}_i = \mathbf{O} + \sigma_i\,[\mathbf{Q}_i - \mathbf{O}] = (1-\sigma_i)\,\mathbf{O} + \sigma_i\,\mathbf{Q}_i \quad (9)$$

for $0 < \sigma_i < 1$.

Consider the generalized cone surface $\mathbf{S}_2(u,v) = \mathbf{O} + v\,[\mathbf{R}(u) - \mathbf{O}]$ where the curve $\mathbf{R}(u)$ is a regular quintic Bézier curve of Equation (4). We pose a plane $\mathbf{\Psi}(t,w) = \mathbf{n} + t\,\mathbf{b} + w\,\mathbf{c}$ between the quintic Bézier curve $\mathbf{R}(u)$ with $0 \leq u \leq 1$ and the point $\mathbf{O}$. Furthermore, the direction of $\mathbf{R}(u)$ and $\mathbf{\Psi}(t,w)$ has the same orientation. By implementing the computation method of Equation (7), the intersection lines at a unique point in the plane $\mathbf{\Psi}$ can be obtained as Equation (10),

$$\mathbf{Q}(u) = \mathbf{O} + \left[\frac{(\mathbf{b}\wedge\mathbf{c}).(\mathbf{n}-\mathbf{O})}{(\mathbf{b}\wedge\mathbf{c}).[\mathbf{R}(u)-\mathbf{O}]}\right][\mathbf{R}(u) - \mathbf{O}] \tag{10}$$

Furthermore, let the control points $[\mathbf{R}_0,\mathbf{R}_1,\mathbf{R}_2,\mathbf{R}_3,\mathbf{R}_4,\mathbf{R}_5]$ of the curve $\mathbf{R}(u)$. Then, the intersection of the lines $\mathbf{O} + v\,[\mathbf{R}_i - \mathbf{O}]$ for $i = 0, 1,\ldots,5$ to the plane $\mathbf{\Psi}(t,w)$ gives $[\mathbf{Q}_0,\mathbf{Q}_1,\mathbf{Q}_2,\mathbf{Q}_3,\mathbf{Q}_4,\mathbf{Q}_5]$ in the forms,

$$\mathbf{Q}_i = \mathbf{O} + \left[\frac{(\mathbf{b}\wedge\mathbf{c}).(\mathbf{n}-\mathbf{O})}{(\mathbf{b}\wedge\mathbf{c}).[\mathbf{R}_i-\mathbf{O}]}\right][\mathbf{R}_i - \mathbf{O}] = \mathbf{O} + \beta_i\,[\mathbf{R}_i - \mathbf{O}] \tag{11}$$

for $0 < \beta_i < 1$. Conversely, if we pose $[\mathbf{Q}_0,\mathbf{Q}_1,\mathbf{Q}_2,\mathbf{Q}_3,\mathbf{Q}_4,\mathbf{Q}_5]$ on the plane $\mathbf{\Psi}$, then, for $i = 0, 1,\ldots,5$, they generate the control points $\mathbf{R}_i$ of the curve $\mathbf{R}(u)$ as follows:

$$\mathbf{R}_i = \mathbf{O} + \delta_i\,[\mathbf{Q}_i - \mathbf{O}] = \mathbf{O} + (\delta_i.\alpha_i)\,[\mathbf{P}_i - \mathbf{O}] \tag{12}$$

where, δ_i, $\alpha_i > 1$.

In regard to Equations (9) and (12), we can state that the points $[\mathbf{O},\mathbf{P}_i,\mathbf{Q}_i,\mathbf{R}_i]$ are consecutively collinear for $i = 0,1,\ldots,5$. Then, for every value u in the interval $0 \leq u \leq 1$, the generatrix lines $\mathbf{O}+[\mathbf{P}(u)-\mathbf{O}]$, $\mathbf{O}+[\mathbf{Q}(u)-\mathbf{O}]$, and $\mathbf{O}+[\mathbf{R}(u)-\mathbf{O}]$ of the cone surface $\mathbf{S}_1(u,v)$ and $\mathbf{S}_2(u,v)$ are coincide with each other. In conclusion, using control points $[\mathbf{Q}_0,\mathbf{Q}_1,\mathbf{Q}_2,\mathbf{Q}_3,\mathbf{Q}_4,\mathbf{Q}_5]$ on the plane $\mathbf{\Psi}$ and the point $\mathbf{O}$ outside the plane $\mathbf{\Psi}$ can define the colinear points $[\mathbf{O},\mathbf{P}_i,\mathbf{Q}_i,\mathbf{R}_i]$ for $i = 0,1,\ldots,5$, such that the cone surface $\mathbf{S}_1(u,v)$ coincide with the cone surface $\mathbf{S}_2(u,v)$. Consequently, when the quintic Bézier curves $[\mathbf{P}(u),\mathbf{R}(u)]$ are placed on different sides of the plane $\mathbf{\Psi}$, through these control points $[\mathbf{Q}_0,\mathbf{Q}_1,\mathbf{Q}_2,\mathbf{Q}_3,\mathbf{Q}_4,\mathbf{Q}_5]$ and the point $\mathbf{O}$ can be constructed the quintic developable Bézier surface using the boundary curves $[\mathbf{P}(u),\mathbf{R}(u)]$ in this way,

$$\begin{aligned}\mathbf{D}(u,v) &= (1-v)\,\mathbf{P}(u) + v\,\mathbf{R}(u)\\ &= (1-v)\sum_{i=0}^{5}[(1-\sigma_i)\mathbf{O} + \sigma_i\mathbf{Q}_i]B_i^5(u) + v\sum_{i=0}^{5}(\mathbf{O} + \delta_i[\mathbf{Q}_i - \mathbf{O}])\,B_i^5(u)\end{aligned} \tag{13}$$

where, $0 < \sigma_i < 1$, $\delta_i > 1$, and $0 \leq u,v \leq 1$.

Based on Equations (9) and (12), we can apply the following numerical procedure to model the quintic developable Bézier surfaces of Equation (13).

(i) Arrange the control points data $[\mathbf{Q}_0,\mathbf{Q}_1,\mathbf{Q}_2,\mathbf{Q}_3,\mathbf{Q}_4,\mathbf{Q}_5]$ of quintic Bézier curve $\mathbf{Q}$(u) in plane $\mathbf{\Psi}$ and the point $\mathbf{O}$ outside this plane $\mathbf{\Psi}$.

(ii) Determine the real values σ_i with $0 < \sigma_i < 1$ for $i = 0, 1,\ldots,5$ for calculating the control points $\mathbf{P}_i = (1-\sigma_i)\,\mathbf{O} + \sigma_i\,\mathbf{Q}_i$ of quintic Bézier curve $\mathbf{P}(u)$.

(iii) Determine δ_i with $\delta_i > 1$ for $i = 0, 1,\ldots,5$ for computing the control points $\mathbf{R}_i = \mathbf{O} + \delta_i\,[\mathbf{Q}_i - \mathbf{O}]$ of quintic Bézier curve $\mathbf{Q}(u)$.

(iv) Construct the curves $\mathbf{P}(u)$ and $\mathbf{Q}(u)$ by using these control points $\mathbf{P}_i$ and $\mathbf{R}_i$ for $i = 0, 1,\ldots,5$, and formulate the quintic developable Bézier surface $\mathbf{D}(u,v)$ of Equation (13).

***Simulation* 1**

In general, in constructing a cone surface shape, we need to define a boundary curve of this surface in plane $\mathbf{\Psi}$ and determine a summit point $\mathbf{O}$ outside $\mathbf{\Psi}$. For this reason, consider the control points that define the quintic Bézier curve $\mathbf{Q}$(u) in the positions $\mathbf{Q}_0$ = <-20,60,20>, $\mathbf{Q}_1$ = <-20,40,40>, $\mathbf{Q}_2$ = <-

20,15,5>, $\mathbf{Q}_3$ = <-20,-15,10>, $\mathbf{Q}_4$ = <-20,-40,80>, $\mathbf{Q}_5$ = <-20,-60,15> and the summit point of the cone surface **O** = <100,10,45>. We choose $\sigma_0 = 2/3$, $\sigma_1 = 5/7$, $\sigma_2 = 2/3$, $\sigma_3 = 3/4$, $\sigma_4 = 2/3$, and $\sigma_5 = 2/3$. Implementing Equation (9) obtains the control points $\mathbf{P}_0$ = <20,130/3,85/3>, $\mathbf{P}_1$ = <100/7,220/7,290/7>, $\mathbf{P}_2$ = <20,40/3,55/3>, $\mathbf{P}_3$ = <10,-35/4,75/4>, $\mathbf{P}_4$ = <20,-70/3,205/3>, $\mathbf{P}_5$ = <20,-110/3,25>. The control point positions $[\mathbf{P}_0,\mathbf{P}_1,\mathbf{P}_2,\mathbf{P}_3,\mathbf{P}_4,\mathbf{P}_5]$ are illustrated in Figure 1. Figure 2 shows the quintic developable Bézier surface that is modeled by two curves $[\mathbf{P}(u),\mathbf{Q}(u)]$ and presents the intersection points between the generatrix lines $\mathbf{O}+v[\mathbf{P}(u)\text{-}\mathbf{O}]$ and the plane $\mathbf{\Psi}$. When we pose the parameters $\sigma_0 = \sigma_1 = \sigma_2 = \sigma_3 = \sigma_4 = \sigma_5 = 2/3$, Figure 3 presents that the control points $[\mathbf{P}_0,\mathbf{P}_1,\mathbf{P}_2,\mathbf{P}_3,\mathbf{P}_4,\mathbf{P}_5]$ and the curve $\mathbf{P}(u)$ are laid in the same plane. Comparing Figure 1 with Figure 3 shows that giving different parameter values to Equation (9) modifies the form of the boundary curve of the surface.

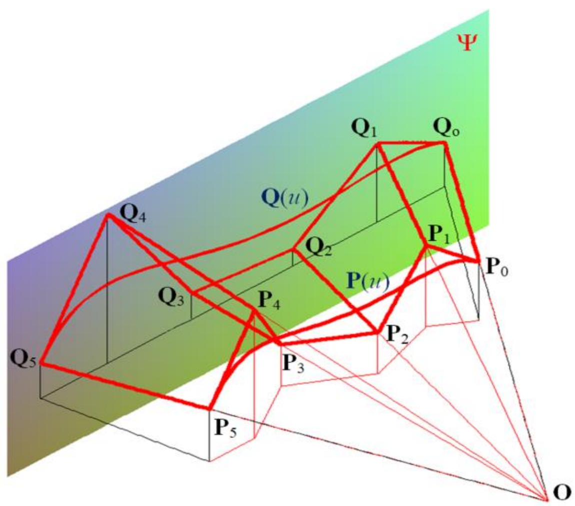

Figure 1. Control point positions of curves $[\mathbf{P}(u), \mathbf{Q}(u)]$.

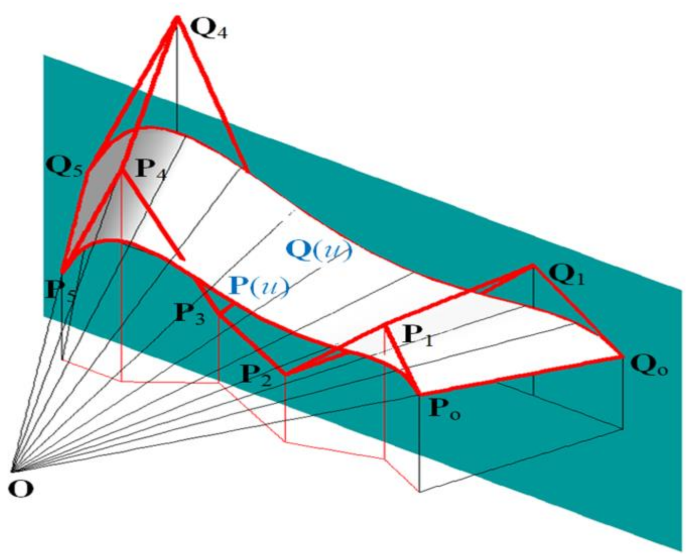

Figure 2. Designing developable Bézier surface through two space curves $[\mathbf{P}(u), \mathbf{Q}(u)]$.

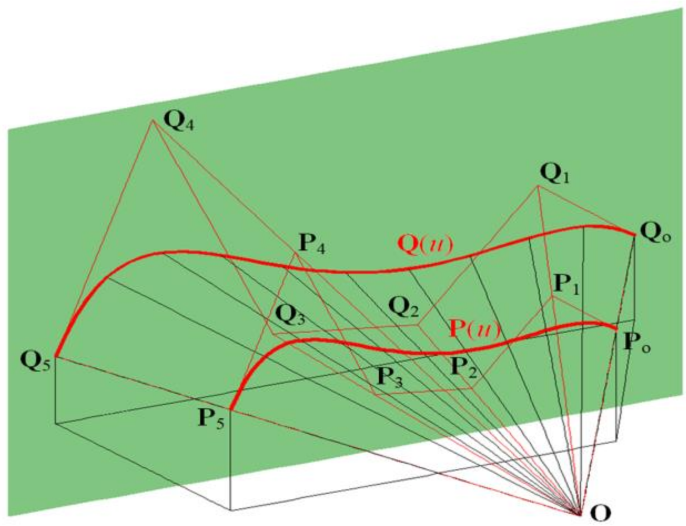

Figure 3. Designing developable Bézier surface through two plane curves [$\mathbf{P}(u)$,$\mathbf{Q}(u)$].

***Simulation* 2**

Choosing data $\mathbf{Q}_0$ = <-20,60,20>, $\mathbf{Q}_1$ = <-20,40,40>, $\mathbf{Q}_2$ = <-20,15,10>, $\mathbf{Q}_3$ = <-20,-15,15>, $\mathbf{Q}_4$ = <-20,-40,80>, $\mathbf{Q}_5$ = <-20,-60,15>, **O** = <100,10,45>, σ_0 = 0.7, σ_1 = 0.84, σ_2 = 0.76, σ_3 = 0.92, σ_4 = 0.82, σ_5 = 0.72, and employing Equation (9) obtain the control points $\mathbf{P}_0$ = <16.4,44.8,27.6>, $\mathbf{P}_1$ = <-0.6,35.2,40.8>, $\mathbf{P}_2$ = <8.8,13.8,18.4>, $\mathbf{P}_3$ = <-10.5,-13,17.4>, $\mathbf{P}_4$ = <2.2,-30.7,73.5>, $\mathbf{P}_5$ = <13.8,-4.3,23.5>. Furthermore, given δ_0 = 1.3, δ_1 = 1.12, δ_2 = 1.2, δ_3 = 1.08, δ_4 = 1.3, δ_5 = 1.28. Applying Equation (12) results $\mathbf{R}_0$ = <-56.4,75.2,12.4>, $\mathbf{R}_1$ = <-34.5,43.6,39.4>, $\mathbf{R}_2$ = <-44,16,3>, $\mathbf{R}_3$ = <-29.5,-17,12.6>, $\mathbf{R}_4$ = <-55.6,-54.8,90.4>, $\mathbf{R}_5$ = <-53.8,-80,6.5>. From these results of control points, using Equation (13) can design the quintic developable Bézier surfaces bounded with the space curves [$\mathbf{P}(u)$,$\mathbf{R}(u)$] in Figure 4.

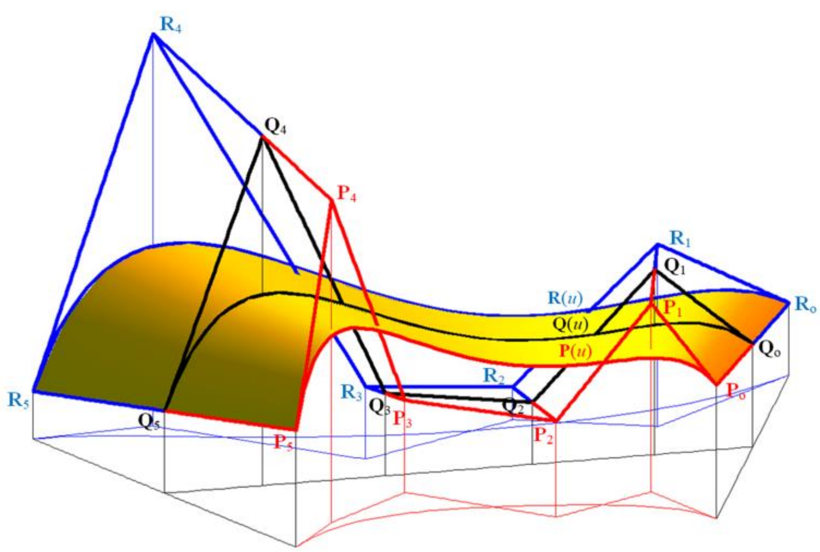

Figure 4. Quintic developable Bézier surface constructed with the curves [$\mathbf{P}(u)$,$\mathbf{R}(u)$].

This computation method provides some advantages in modeling the developable surfaces. In plane $\mathbf{\Psi}$, we can easily set the control points $[\mathbf{Q}_0,\mathbf{Q}_1,\mathbf{Q}_2,\mathbf{Q}_3,\mathbf{Q}_4,\mathbf{Q}_5]$ for raising, lowering, or changing arches of the curve $\mathbf{Q}(u)$ to model the various shapes (fluctuations) of the developable surfaces. In general, it can be used to design the developable surface in three different arches of surface shape (Figure 2 and Figure 4). Determining σ_i and δ_i for Equation (13) with $0 < \sigma_i < 1$ and $\delta_i > 1$ for $i = 0, 1,\ldots,5$, can effectively modify and adjust the desired profile of the boundary curves $[\mathbf{P}(u),\mathbf{R}(u)]$ of these surfaces.

2.2 Quintic Developable Bézier Surfaces Defined with Generalized Cylinder Surface

Suppose we have the generalized cylinder surface $\mathbf{S}_1(u,v) = \mathbf{P}(u) - v\,\mathbf{U}$. The curve $\mathbf{P}(u)$ of Equation (4) is placed outside a plane $\mathbf{\Psi}(t,w) = \mathbf{n} + t\,\mathbf{b} + w\,\mathbf{c}$. We restrict that the direction of this curve and plane $\mathbf{\Psi}$ are in the same orientation. For every point $\mathbf{P}(a)$ on the curve $\mathbf{P}(u)$ with the real value a in the interval $0 \le a \le 1$, the prolongation of line $\mathbf{P}(a) + v\,\mathbf{U}$ intersects at a unique point on plane $\mathbf{\Psi}$.

$$\mathbf{Q}(v) = \mathbf{P}(a) + v\,\mathbf{U} = \mathbf{n} + t\,\mathbf{b} + w\,\mathbf{c} \tag{14}$$

We find the scalar v in form $v = \frac{(\mathbf{b}\wedge\mathbf{c}).[\mathbf{n}-\mathbf{P}(a)]}{(\mathbf{b}\wedge\mathbf{c}).\mathbf{U}}$. Thus, the intersection points $\mathbf{Q}(u)$ on this plane $\mathbf{\Psi}$ are,

$$\mathbf{Q}(u) = \mathbf{P}(u) + \left[\frac{(\mathbf{b}\wedge\mathbf{c}).[\mathbf{n}-\mathbf{P}(u)]}{(\mathbf{b}\wedge\mathbf{c}).\mathbf{U}}\right]\mathbf{U}.$$

In conclusion, using control points data $[\mathbf{P}_0,\mathbf{P}_1,\mathbf{P}_2,\mathbf{P}_3,\mathbf{P}_4,\mathbf{P}_5]$ of space curve $\mathbf{P}(u)$ sets the intersection control points $[\mathbf{Q}_0,\mathbf{Q}_1,\mathbf{Q}_2,\mathbf{Q}_3,\mathbf{Q}_4,\mathbf{Q}_5]$ in plane Ψ through the following equations for $i = 0, 1,\ldots,5$.

$$\mathbf{Q}_i = \mathbf{P}_i + \left[\frac{(\mathbf{b}\wedge\mathbf{c}).[\mathbf{n}-\mathbf{P}_i]}{(\mathbf{b}\wedge\mathbf{c}).\mathbf{U}}\right]\mathbf{U} = \mathbf{P}_i + \alpha_i\,\mathbf{U} \tag{15}$$

where, $\alpha_i > 0$. Conversely, using the points $[\mathbf{Q}_0,\mathbf{Q}_1,\mathbf{Q}_2,\mathbf{Q}_3,\mathbf{Q}_4,\mathbf{Q}_5]$ on plane $\mathbf{\Psi}$, we determine the control points $[\mathbf{P}_0,\mathbf{P}_1,\mathbf{P}_2,\mathbf{P}_3,\mathbf{P}_4,\mathbf{P}_5]$ of the curve $\mathbf{P}(u)$ as follows:

$$\mathbf{P}_i = \mathbf{Q}_i - \alpha_i\,\mathbf{U} \tag{16}$$

Consider the generalized cylinder surface $\mathbf{S}_2(u,v) = \mathbf{R}(u) - v\,\mathbf{U}$. The curve $\mathbf{R}(u)$ is a regular quintic Bézier curve of control points $[\mathbf{R}_0,\mathbf{R}_1,\mathbf{R}_2,\mathbf{R}_3,\mathbf{R}_4,\mathbf{R}_5]$. In this case, the curves $\mathbf{R}(u)$ and $\mathbf{P}(u)$ are laid on different sides of plane $\mathbf{\Psi}$. Also, the intersection between the lines $\mathbf{R}_i - v\,\mathbf{U}$ and the plane $\mathbf{\Psi}$ for $i = 0, 1,\ldots,5$ obtains the control points $[\mathbf{Q}_0,\mathbf{Q}_1,\mathbf{Q}_2,\mathbf{Q}_3,\mathbf{Q}_4,\mathbf{Q}_5]$ in the form,

$$\mathbf{Q}_i = \mathbf{R}_i - \left[\frac{(\mathbf{b}\wedge\mathbf{c}).[\mathbf{n}-\mathbf{R}_i]}{(\mathbf{b}\wedge\mathbf{c}).\mathbf{U}}\right]\mathbf{U} = \mathbf{R}_i - \beta_i\,\mathbf{U}.$$

where, the real scalars $\beta_i > 0$. Conversely, if we arrange the control points $[\mathbf{Q}_0,\mathbf{Q}_1,\mathbf{Q}_2,\mathbf{Q}_3,\mathbf{Q}_4,\mathbf{Q}_5]$ on plane $\mathbf{\Psi}$, then, for $i = 0, 1,\ldots,5$, we find,

$$\mathbf{R}_i = \mathbf{Q}_i + \beta_i\,\mathbf{U} = \mathbf{P}_i + (\alpha_i + \beta_i)\,\mathbf{U} \tag{17}$$

where $\alpha_i, \beta_i > 0$.

Based on Equations (16) and (17), the points $[\mathbf{P}_i,\mathbf{Q}_i,\mathbf{R}_i]$ are successively collinear for $i = 0,1,\ldots,5$. In addition, for every value u in the interval $0 \le u \le 1$, the generatrix lines $[\mathbf{Q}(u)\text{-}\mathbf{P}(u)]$ and $[\mathbf{R}(u)\text{-}\mathbf{P}(u)]$ of the cylinder surface $\mathbf{S}_1(u,v)$ and $\mathbf{S}_2(u,v)$ are coincide with each other and parallel to the vector $\mathbf{U}$. Therefore, using data $[\mathbf{Q}_0,\mathbf{Q}_1,\mathbf{Q}_2,\mathbf{Q}_3,\mathbf{Q}_4,\mathbf{Q}_5]$ on the plane $\mathbf{\Psi}$ can design the cylinder surface limited by the quintic Bézier curves $[\mathbf{P}(u),\mathbf{R}(u)]$ that are placed in the different side of the plane $\mathbf{\Psi}$ in this fashion,

$$\mathbf{D}(u,v) = (1\text{-}v)\, \mathbf{P}(u) + v\, \mathbf{R}(u)$$
$$= (1\text{-}v) \sum_{i=0}^{5}(\mathbf{Q}_i - \alpha_i \mathbf{U}) B_i^5(u) + v \sum_{i=0}^{5}(\mathbf{Q}_i + \beta_i \mathbf{U})\, B_i^5(u) \quad (18)$$

where, α_i, $\beta_i > 0$.

In general, designing the cylinder surface limited with the quintic Bézier curves [$\mathbf{P}(u)$,$\mathbf{R}(u)$] can be conducted in steps: (a) arranging the control points' data $\mathbf{Q}_i$ in the plane $\mathbf{\Psi}$, the parameter values α_i, $\beta_i > 0$ for i = 0, 1,…,5, and fixing nonzero direction vector **U** unparallel to this plane $\mathbf{\Psi}$; (b) Implementing the Equations (16), (17), and computing the control points $\mathbf{P}_i$ and $\mathbf{R}_i$; and (c) plotting the quintic developable Bézier surface $\mathbf{D}(u,v)$ by using Equation (18).

***Simulation* 3**

Based on the steps of the cylinder surface construction, we can design the surface through a quintic Bézier curve $\mathbf{Q}(u)$ and a fixed nonzero direction vector **U** with the following data. Let the control points' data $\mathbf{Q}_0$ = <-20,60,30>, $\mathbf{Q}_1$ = <-20,40,50>, $\mathbf{Q}_2$ = <-20,15,15>, $\mathbf{Q}_3$ = <-20,-5,20>, $\mathbf{Q}_4$ = <-20,-40,70>, $\mathbf{Q}_5$ = <-20,-60,25>, and we determine the nonzero direction vector and parameter values **U** = <-2/√6, 1/√6, 1/√6>, α_0 = 20, α_1 = 40, α_2 = 30, α_3 = 45, α_4 = 15, α_5 = 40. By implementing Equation (16), we get the control points $\mathbf{P}_0$ = <-3.7,51.8,21.8>, $\mathbf{P}_1$ = <12.7,23.7,33.7>, $\mathbf{P}_2$ = <4.5,2.8,2.8>, $\mathbf{P}_3$ = <16.7,-33.4,1.6>, $\mathbf{P}_4$ = <-7.8,-46.7,63.9>, $\mathbf{P}_5$ = <12.7,-76.3,8.7> as shown in Figure 5. These calculated data present the quintic developable Bézier surface of the cylinder surface type.

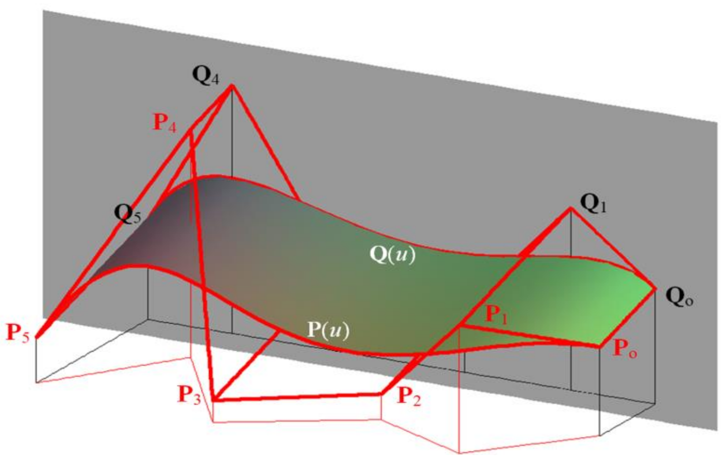

Figure 5. The quintic Bézier curve $\mathbf{P}(u)$ with the control points [$\mathbf{P}_0$, $\mathbf{P}_1$, $\mathbf{P}_2$, $\mathbf{P}_3$, $\mathbf{P}_4$, $\mathbf{P}_5$].

***Simulation* 4**

In the same way as simulation 3, arranging the data $\mathbf{Q}_0$ = <-20,60,30>, $\mathbf{Q}_1$ = <-20,40,50>, $\mathbf{Q}_2$ = <-20,15,20>, $\mathbf{Q}_3$ = <-20,-15,25>, $\mathbf{Q}_4$ = <-20,-40,70>, $\mathbf{Q}_5$ = <-20,-60,25>, **U** = <-2/√6, 1/√6, 1/√6>, α_0 = 20, α_1 = 40, α_2 = 30, α_3 = 45, α_4 = 15, α_5 = 40. By implementing Equation (18), we obtain the control points $\mathbf{P}_0$ = <-3.7,51.8,21.8>, $\mathbf{P}_1$ = <12.7,23.7,33.7>, $\mathbf{P}_2$ = <4.5,2.8,7.8>, $\mathbf{P}_3$ = <16.7,-33.4,6.6>, $\mathbf{P}_4$ = <-7.8,-46.1,63.9>, $\mathbf{P}_5$ = <12.7,-76.3,8.7>. On the other hand, given β_0 =20, β_1 =35, β_2 =15, β_3 =10, β_4 =30, β_5 =30. Computing Equation (17) obtains $\mathbf{R}_0$ = <-36.3,68.1,38.2>, $\mathbf{R}_1$ = <-48.6,54.3,64.3>, $\mathbf{R}_2$ = <-32.2,21.1,26.1>, $\mathbf{R}_3$ = <-28.1,-10.9,29.1>, $\mathbf{R}_4$ = <-44.5,-27.6,82.2>, $\mathbf{R}_5$ = <-44.5,-47.8,37.2>. These calculation data give the quintic developable Bézier surface bounded with the space curves [$\mathbf{P}(u)$, $\mathbf{R}(u)$] as given in Figure 6. Evaluating Figure 5 and Figure 6 can be stated that, by determining the parameters α_i and β_i for i = 0, 1,…,5, the developable surfaces' boundary curves can be situated in space.

This computational approach offers some efficacities in designing the surfaces. The election [$\mathbf{Q}_0$,$\mathbf{Q}_1$,$\mathbf{Q}_2$,$\mathbf{Q}_3$,$\mathbf{Q}_4$,$\mathbf{Q}_5$] on plane $\mathbf{\Psi}$ can easily change curve $\mathbf{Q}(u)$ arches and the developable surface shape. Substituting real values α_i and β_i for i = 0, 1,…,5 to Equation (18) can model the developable surfaces' boundary curves [$\mathbf{P}(u)$,$\mathbf{R}(u)$] laid in space.

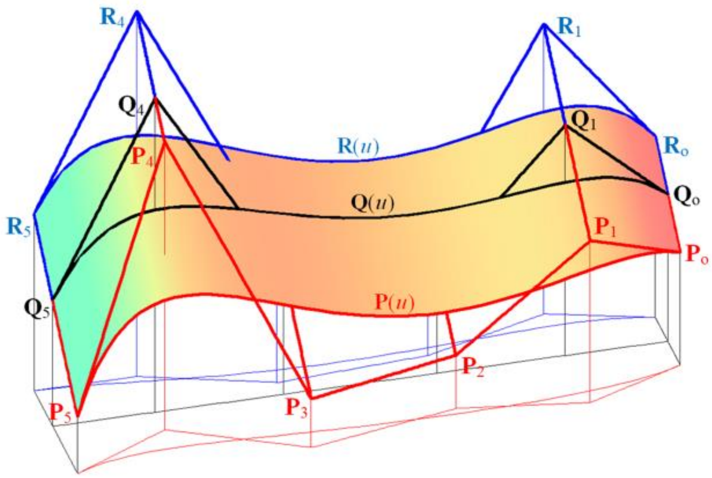

Figure 6. Designing Bézier cylinder surface of the boundary curves [$\mathbf{P}(u)$, $\mathbf{R}(u)$].

3. Quintic Developable Hermite Surfaces Construction

We describe the mathematical theory for presenting the equation of a quintic Hermite curve defined by the boundary conditions. After that, we offer a new approach to model the quintic developable Hermite surface. Finally, we simulate this result using the mathematics software.

Suppose a quintic polynomial curve $\mathbf{P}(u) = \mathbf{a}_5 u^5 + \mathbf{a}_4 u^4 + \mathbf{a}_3 u^3 + \mathbf{a}_2 u^2 + \mathbf{a}_1 u + \mathbf{a}_0$ with the restrictions at the points $\mathbf{P}(0) = \mathbf{P}_o$, $\mathbf{P}(1) = \mathbf{P}_1$, two intermediate points $\mathbf{P}(1/3) = \mathbf{P}_{1/3}$ and $\mathbf{P}(2/3) = \mathbf{P}_{2/3}$, and two tangent vectors value $\mathbf{P}^u(0) = \mathbf{P}_o^u$, $\mathbf{P}^u(1) = \mathbf{P}_1^u$. Computing the equations of these six limitations and evaluating the unknown coefficients value $\mathbf{a}_5$, $\mathbf{a}_4$, $\mathbf{a}_3$, $\mathbf{a}_2$, $\mathbf{a}_1$, and $\mathbf{a}_0$ of the curve $\mathbf{P}(u)$, the definition of quintic Hermite curve $\mathbf{P}(u)$ is (Kusno, 2020a),

$$\mathbf{P}(u) = F_1(u)\,\mathbf{P}_o + F_2(u)\,\mathbf{P}_{1/3} + F_3(u)\,\mathbf{P}_{2/3} + F_4(u)\,\mathbf{P}_1 + F_5(u)\,\mathbf{P}_o^u + F_6(u)\mathbf{P}_1^u \quad (19)$$

where, the real functions (scalars),

$F_1(u) = 29.25u^5 - 83.25u^4 + 80.75u^3 - 27.75u^2 + 1$; $F_2(u) = -60.75u^5 + 162u^4 - 141.75u^3 + 40.5u^2$;
$F_3(u) = 60.75u^5 - 141.75u^4 + 101.25u^3 - 20.25u^2$; $F_4(u) = -29.25u^5 + 63u^4 - 40.25u^3 + 7.5u^2$;
$F_5(u) = 4.5u^5 - 13.5u^4 + 14.5u^3 - 6.5u^2 + u$; $F_6(u) = 4.5u^5 - 9u^4 + 5.5u^3 - u^2$.

In constructing quintic developable Hermite surfaces of cone type $\mathbf{S}_1(u,v) = \mathbf{O} + v\,[\mathbf{P}(u) - \mathbf{O}]$, we give the restrictions that the quintic Hermite curve $\mathbf{P}(u)$ is positioned between the fixed point $\mathbf{O}$ and a plane $\mathbf{\Psi}(t,w) = \mathbf{n} + t\,\mathbf{b} + w\,\mathbf{c}$. In addition, the direction of $\mathbf{P}(u)$ and $\mathbf{\Psi}(t,w)$ are in the same orientation. Based on this criteria, let a point $\mathbf{P}_x$ be any control points [$\mathbf{P}_o$,$\mathbf{P}_{1/3}$,$\mathbf{P}_{2/3}$,$\mathbf{P}_1$] of the quintic Hermite curve $\mathbf{P}(u)$ in Equation (19). Prolonging line $\mathbf{O} + v\,[\mathbf{P}_x - \mathbf{O}]$ from the point $\mathbf{O}$ to the plane $\mathbf{\Psi}$ intersects at a unique control point $\mathbf{Q}_x$ on this plane $\mathbf{\Psi}$ (that represents any control points [$\mathbf{Q}_o$,$\mathbf{Q}_{1/3}$,$\mathbf{Q}_{2/3}$,$\mathbf{Q}_1$]) in the calculation.

$$\mathbf{Q}_x = \mathbf{O} + \left[\frac{(\mathbf{b}\wedge\mathbf{c}).(\mathbf{n}-\mathbf{O})}{(\mathbf{b}\wedge\mathbf{c}).[\mathbf{P}_x-\mathbf{O}]}\right][\mathbf{P}_x - \mathbf{O}] = \mathbf{O} + \alpha_x\,[\mathbf{P}_x - \mathbf{O}] \quad (20)$$

where, $\alpha_x > 1$. From the tangent vectors $[\mathbf{P}_o^u, \mathbf{P}_1^u]$, we can compute the tangent vectors $[\mathbf{Q}_o^u, \mathbf{Q}_1^u]$ in the plane $\mathbf{\Psi}$ as follows (Figure 7).

$$\mathbf{Q}_0^u = \left[\frac{(\mathbf{b}\wedge\mathbf{c}).(\mathbf{n}-\mathbf{O})}{(\mathbf{b}\wedge\mathbf{c}).[(\mathbf{P}_0-\mathbf{O})+\mathbf{P}_0^u]}\right] [(\mathbf{P}_0-\mathbf{O}) + \mathbf{P}_0^u] - (\mathbf{Q}_0-\mathbf{O}) \tag{21}$$
$$= \Omega_0 [(\mathbf{P}_0-\mathbf{O}) + \mathbf{P}_0^u] - (\mathbf{Q}_0-\mathbf{O}).$$

$$\mathbf{Q}_1^u = \left[\frac{(\mathbf{b}\wedge\mathbf{c}).(\mathbf{n}-\mathbf{O})}{(\mathbf{b}\wedge\mathbf{c}).[(\mathbf{P}_1-\mathbf{O})+\mathbf{P}_1^u]}\right] [(\mathbf{P}_1-\mathbf{O}) + \mathbf{P}_1^u] - (\mathbf{Q}_1-\mathbf{O}) \tag{22}$$
$$= \Omega_1 [(\mathbf{P}_1-\mathbf{O}) + \mathbf{P}_1^u] - (\mathbf{Q}_1-\mathbf{O}).$$

where, $\Omega_0, \Omega_1 > 1$. Thus, it can state that,

$$\mathbf{P}_x = \mathbf{O} + \sigma_x [\mathbf{Q}_x - \mathbf{O}] = (1-\sigma_x)\, \mathbf{O} + \sigma_x \mathbf{Q}_x \tag{23}$$
$$\mathbf{P}_0^u = \rho_0 [(\mathbf{Q}_0-\mathbf{O}) + \mathbf{Q}_0^u] - (\mathbf{P}_0-\mathbf{O}) = \rho_0 [(\mathbf{Q}_0-\mathbf{O}) + \mathbf{Q}_0^u] - \sigma_0 [\mathbf{Q}_0-\mathbf{O}] \tag{24}$$
$$\mathbf{P}_1^u = \rho_1 [(\mathbf{Q}_1-\mathbf{O}) + \mathbf{Q}_1^u] - (\mathbf{P}_1-\mathbf{O}) = \rho_1 [(\mathbf{Q}_1-\mathbf{O}) + \mathbf{Q}_1^u] - \sigma_1 [\mathbf{Q}_1-\mathbf{O}] \tag{25}$$

where, $0 < \sigma_x < 1$, and $0 < \rho_0, \rho_1 < 1$.

Consider a developable surface of cone type $\mathbf{S}_2(u,v) = \mathbf{O} + v\,[\mathbf{R}(u) - \mathbf{O}]$ with the plane $\mathbf{\Psi}(t,w)$ laid between the fixed point $\mathbf{O}$ and the quintic Hermite curve $\mathbf{R}(u)$. Moreover, for a control point $\mathbf{R}_x$ that represents any control points $[\mathbf{R}_o,\mathbf{R}_{1/3},\mathbf{R}_{2/3},\mathbf{R}_1]$ of the curve $\mathbf{R}(u)$, the line $\mathbf{O} + v\,[\mathbf{R}_x - \mathbf{O}]$ intersects at a unique control point $\mathbf{Q}_x$ on the plane $\mathbf{\Psi}$ (that represents any control points $[\mathbf{Q}_o,\mathbf{Q}_{1/3},\mathbf{Q}_{2/3},\mathbf{Q}_1]$) of the equation (Figure 8),

$$\mathbf{Q}_x = \mathbf{O} + \left[\frac{(\mathbf{b}\wedge\mathbf{c}).(\mathbf{n}-\mathbf{O})}{(\mathbf{b}\wedge\mathbf{c}).[\mathbf{R}_x-\mathbf{O}]}\right] [\mathbf{R}_x - \mathbf{O}] = \mathbf{O} + \beta_x [\mathbf{R}_x - \mathbf{O}] \tag{26}$$

where, $0 < \beta_x < 1$. Then, the tangent vectors $[\mathbf{R}_o^u, \mathbf{R}_1^u]$ determine the tangent vectors $[\mathbf{Q}_o^u, \mathbf{Q}_1^u]$ in plane $\mathbf{\Psi}$,

$$\mathbf{Q}_0^u = \left[\frac{(\mathbf{b}\wedge\mathbf{c}).(\mathbf{n}-\mathbf{O})}{(\mathbf{b}\wedge\mathbf{c}).((\mathbf{R}_0-\mathbf{O})+\mathbf{R}_0^u)}\right] [(\mathbf{R}_0-\mathbf{O}) + \mathbf{R}_0^u] - (\mathbf{Q}_0-\mathbf{O}) \tag{27}$$
$$= \xi_0 [(\mathbf{R}_0-\mathbf{O}) + \mathbf{R}_0^u] - (\mathbf{Q}_0-\mathbf{O}).$$

$$\mathbf{Q}_1^u = \left[\frac{(\mathbf{a}-\mathbf{O}).(\mathbf{n}\wedge\mathbf{d})}{(\mathbf{b}\wedge\mathbf{c}).((\mathbf{R}_1-\mathbf{O})+\mathbf{R}_1^u)}\right] [(\mathbf{R}_1-\mathbf{O}) + \mathbf{R}_1^u] - (\mathbf{Q}_1-\mathbf{O}) \tag{28}$$
$$= \xi_1 [(\mathbf{R}_1-\mathbf{O}) + \mathbf{R}_1^u] - (\mathbf{Q}_1-\mathbf{O}).$$

where, $0 < \xi_0, \xi_1 < 1$. Therefore, we can state that,

$$\mathbf{R}_x = \mathbf{O} + \delta_x [\mathbf{Q}_x - \mathbf{O}] = \mathbf{O} + \delta_x.\alpha_x [\mathbf{P}_x - \mathbf{O}] \tag{29}$$
$$\mathbf{R}_0^u = \tau_0 [(\mathbf{Q}_0-\mathbf{O}) + \mathbf{Q}_0^u] - (\mathbf{R}_0-\mathbf{O}) = \tau_0 [(\mathbf{Q}_0-\mathbf{O}) + \mathbf{Q}_0^u] - \delta_0 [\mathbf{Q}_0 - \mathbf{O}] \tag{30}$$
$$\mathbf{R}_1^u = \tau_1 [(\mathbf{Q}_1-\mathbf{O}) + \mathbf{Q}_1^u] - (\mathbf{R}_1-\mathbf{O}) = \tau_1 [(\mathbf{Q}_0-\mathbf{O}) + \mathbf{Q}_1^u] - \delta_1 [\mathbf{Q}_1 - \mathbf{O}] \tag{31}$$

where, $\delta_x, \alpha_x > 1$, and $\tau_0, \tau_1 > 1$.

From Equations (23), (24), (25), (22), (29), (30), and (31), the points $[\mathbf{O},\mathbf{P}_x,\mathbf{Q}_x,\mathbf{R}_x]$ are colinear, and the tangent vectors $[\mathbf{P}_0^u,\mathbf{Q}_0^u,\mathbf{R}_0^u]$, and $[\mathbf{P}_1^u, \mathbf{Q}_1^u,\mathbf{R}_1^u]$ are respectively coplanar in the tangent planes $[\mathbf{Q}_0^u,(\mathbf{Q}_0-\mathbf{O})]$ and $[\mathbf{Q}_1^u,(\mathbf{Q}_1-\mathbf{O})]$. Thus, the generatrix lines $\mathbf{O}+[\mathbf{P}(u)-\mathbf{O}]$ and $\mathbf{O}+[\mathbf{R}(u)-\mathbf{O}]$ of the cone surfaces $\mathbf{S}_1(u,v)$ and $\mathbf{S}_2(u,v)$ are respectively in a line for every value u in the interval $0 \leq u \leq 1$. Thus, the developable surfaces

$\mathbf{S}_1(u,v)$ and $\mathbf{S}_2(u,v)$ coincide. Consequently, the generalized cone surface that is limited by the Hermite curves $[\mathbf{P}(u),\mathbf{R}(u)]$ is,

$$\begin{aligned}\mathbf{D}(u,v) &= (1-v)\,\mathbf{P}(u) + v\,\mathbf{R}(u)\\ &= (1-v)\,\{F_1(u)\,(\mathbf{O} + \sigma_0[\mathbf{Q}_0-\mathbf{O}]) + F_2(u)\,(\mathbf{O} + \sigma_{1/3}[\mathbf{Q}_{1/3}-\mathbf{O}]) + F_3(u)\,(\mathbf{O} + \sigma_{2/3}[\mathbf{Q}_{2/3}-\mathbf{O}]) +\\ &\quad F_4(u)\,(\mathbf{O} + \sigma_1[\mathbf{Q}_1-\mathbf{O}]) + F_5(u)\,(\rho_0[(\mathbf{Q}_0 - \mathbf{O}) + \mathbf{Q}_0^u] - \sigma_0(\mathbf{Q}_0 - \mathbf{O})) +\\ &\quad F_6(u)\,(\rho_1[(\mathbf{Q}_1 - \mathbf{O}) + \mathbf{Q}_1^u] - \sigma_1(\mathbf{Q}_1 - \mathbf{O}))\} +\\ &\quad v\,\{F_1(u)\,(\mathbf{O} + \delta_0[\mathbf{Q}_0-\mathbf{O}]) + F_2(u)\,(\mathbf{O} + \delta_{1/3}[\mathbf{Q}_{1/3}-\mathbf{O}]) + F_3(u)\,(\mathbf{O} + \delta_{2/3}[\mathbf{Q}_{2/3}-\mathbf{O}]) +\\ &\quad F_4(u)\,(\mathbf{O} + \delta_1[\mathbf{Q}_1-\mathbf{O}]) + F_5(u)\,(\tau_0\,[(\mathbf{Q}_0 - \mathbf{O}) + \mathbf{Q}_0^u] - \delta_0\,[\mathbf{Q}_0 - \mathbf{O}]) +\\ &\quad F_6(u)\,(\tau_1\,[(\mathbf{Q}_1 - \mathbf{O}) + \mathbf{Q}_1^u] - \delta_1\,[\mathbf{Q}_1 - \mathbf{O}])\}\end{aligned} \tag{32}$$

where, $0 < \sigma_0, \sigma_{1/3}, \sigma_{2/3}, \sigma_1, \rho_0, \rho_1 < 1$; $\delta_0, \delta_{1/3}, \delta_{2/3}, \delta_1, \tau_0, \tau_1 > 1$; and $0 \le u,v \le 1$.

Based on Equation (32), modeling quintic developable Hermite surfaces $\mathbf{D}(u,v)$ of generalized cone type in Equation (3) can employ the following numerical procedure.

(i) Arrange the control points data $[\mathbf{Q}_0,\mathbf{Q}_{1/3},\mathbf{Q}_{2/3},\mathbf{Q}_1]$ and two tangent vectors $[\mathbf{Q}_0^u,\mathbf{Q}_1^u]$ of quintic Hermite curve $\mathbf{Q}(u)$ in plane $\mathbf{\Psi}$ and a point $\mathbf{O}$ outside plane $\mathbf{\Psi}$ (Figure 7).

(ii) Calculate the control points $\mathbf{P}_0$, $\mathbf{P}_{1/3}$, $\mathbf{P}_{2/3}$, $\mathbf{P}_1$, and the tangent vectors $\mathbf{P}_0^u$, $\mathbf{P}_1^u$ using Equations (23), (24), and (25) for the quintic Hermite curve $\mathbf{P}(u)$, and compute the control points $\mathbf{R}_0$, $\mathbf{R}_{1/3}$, $\mathbf{R}_{2/3}$, $\mathbf{R}_1$, and the tangent vectors $\mathbf{R}_0^u$, $\mathbf{R}_1^u$ utilizing Equations (29), (30), and (31) for the quintic Hermite curve $\mathbf{R}(u)$.

(iii) Plote the quintic developable Hermite surface $\mathbf{D}(u,v)$ using Equation (32).

***Simulation* 5**

Setting data $\mathbf{Q}_0$ = <-20,70,40>, $\mathbf{Q}_{1/3}$ = <-20,10,20>, $\mathbf{Q}_{2/3}$ = <-20,-30,30>, $\mathbf{Q}_1$ = <-20,-90,20>, $\mathbf{Q}_0^u$ = <0,-70,-90>, $\mathbf{Q}_1^u$ = <0,-40,-70>, $\mathbf{O}$ = <120,10,45>, σ_0 =0.68, $\sigma_{1/3}$ =0.72, $\sigma_{2/3}$ =0.80, σ_1 =0.71, ρ_0 =7/10, ρ_1 =7/10, and utilizing Equations (23), (24) and (25) obtain the control points $\mathbf{P}_0$ = <26.1,50.3,41.6>, $\mathbf{P}_{1/3}$ = <19.4,10,27>, $\mathbf{P}_{2/3}$ = <4,-23.2,32.6>, $\mathbf{P}_1$ = <20.2,-61.3,27.2>, and the tangent vectors $\mathbf{P}_0^u$ = <24,-45.3,-44.1>, $\mathbf{P}_1^u$ = <1.8,-26.7,-48.7>. Employing the data and Equation (32), we can construct the quintic developable Hermite surface that is presented in Figure 7. Then, given δ_0 =1.2, $\delta_{1/3}$ =1.4, $\delta_{2/3}$ =1.2, δ_1 =1.2, τ_0 =1.2, τ_1 =1.3. Calculating Equations (29), (30), and (31) obtain $\mathbf{R}_0$ = <-47.6,81.8,39>, $\mathbf{R}_{1/3}$ = <-74.2,10,10.3>, $\mathbf{R}_{2/3}$ = <-53.6,-39.6,26.4>, $\mathbf{R}_1$ = <-44.1,-107.2,15.7>, $\mathbf{R}_0^u$ = <-0.4,-83.8,-108>, $\mathbf{R}_1^u$ = <-17.9,-64.8,-94.2>. Using the control points $[\mathbf{P}_0,\mathbf{P}_{1/3},\mathbf{P}_{2/3},\mathbf{P}_1]$, $[\mathbf{R}_0,\mathbf{R}_{1/3},\mathbf{R}_{2/3},\mathbf{R}_1]$, and Equation (32) can design the quintic developable Hermite surfaces placed between the space curves $[\mathbf{P}(u),\mathbf{R}(u)]$ as shown in Figure 8. Figure 9 shows the positions of the tangent vectors $[\mathbf{P}_0^u,\mathbf{P}_1^u]$ and $[\mathbf{R}_0^u,\mathbf{R}_1^u]$. Figure 10 illustrates the boundary curves profile of the surface.

In modeling the quintic developable Hermite surface of cylinder surface $\mathbf{S}_1(u,v) = \mathbf{P}(u) + v\,\mathbf{U}$, we use the same restriction of the cone surface type. From this condition, consider a point $\mathbf{P}_x$ that expresses any control points $[\mathbf{P}_o,\mathbf{P}_{1/3},\mathbf{P}_{2/3},\mathbf{P}_1]$ of the quintic Hermite curve $\mathbf{P}(u)$ in Equation (19). The extension of line $\mathbf{P}_x + v\,\mathbf{U}$ to plane $\mathbf{\Psi}$ intersects this plane $\mathbf{\Psi}$ at a unique control point $\mathbf{Q}_x$ (that represents any control points $[\mathbf{Q}_o,\mathbf{Q}_{1/3},\mathbf{Q}_{2/3},\mathbf{Q}_1]$) in the form,

$$\mathbf{Q}_x = \mathbf{P}_x + \alpha_x\,\mathbf{U} \tag{33}$$

for $\alpha_x > 0$. In addition, their tangent planes are constant for all points of a generator line of this surface.

Thus, the tangent vectors $[\mathbf{P}_o^u, \mathbf{P}_1^u]$ result the tangent vectors $[\mathbf{Q}_o^u, \mathbf{Q}_1^u]$ such that the vectors $[\mathbf{P}_o^u, \mathbf{Q}_o^u]$ and $[\mathbf{P}_1^u, \mathbf{Q}_1^u]$ are respectively in the same plane tangent $[\mathbf{P}_o^u, \mathbf{U}]$ and $[\mathbf{P}_1^u,\mathbf{U}]$. The tangent vectors $[\mathbf{Q}_o^u, \mathbf{Q}_1^u]$ are,

$\mathbf{Q}_0^u = \mathbf{P}_0^u + \rho_0\,\mathbf{U}$ (34)
$\mathbf{Q}_1^u = \mathbf{P}_1^u + \rho_1\,\mathbf{U}$ (35)

where, $\rho_0, \rho_1 > 0$. Thus, we can state that,
$\mathbf{P}_x = \mathbf{Q}_x - \alpha_x\,\mathbf{U}$; $\mathbf{P}_0^u = \mathbf{Q}_0^u - \rho_0\,\mathbf{U}$; $\mathbf{P}_1^u = \mathbf{Q}_1^u - \rho_1\,\mathbf{U}$ (36)

Besides, let a developable surface of cylinder type $\mathbf{S}_2(u,v) = \mathbf{R}(u) + v\,\mathbf{U}$, and $\mathbf{R}(u)$ the quintic Hermite curve. For a control point $\mathbf{R}_x$ that represents any control points $[\mathbf{R}_o,\mathbf{R}_{1/3},\mathbf{R}_{2/3},\mathbf{R}_1]$ of the curve $\mathbf{R}(u)$, the line $\mathbf{R}_x + v\,\mathbf{U}$ intersects the plane $\mathbf{\Psi}$ at a unique control point $\mathbf{Q}_x$ (that represents any control points $[\mathbf{Q}_o,\mathbf{Q}_{1/3},\mathbf{Q}_{2/3},\mathbf{Q}_1]$) as follows:
$\mathbf{Q}_x = \mathbf{R}_x - \beta_x\,\mathbf{U}$ (37)

where, $\beta_x > 0$. Then, the tangent vectors $[\mathbf{R}_o^u, \mathbf{R}_1^u]$ generate the tangent vectors $[\mathbf{Q}_o^u, \mathbf{Q}_1^u]$ in the form,
$\mathbf{Q}_0^u = \mathbf{R}_0^u - \tau_0\,\mathbf{U}$ (38)
$\mathbf{Q}_1^u = \mathbf{R}_1^u - \tau_1\,\mathbf{U}$ (39)

where, $\tau_0, \tau_1 > 0$. Therefore, we can state that,
$\mathbf{R}_x = \mathbf{Q}_x + \beta_x\,\mathbf{U}$; $\mathbf{R}_0^u = \mathbf{Q}_0^u + \tau_0\,\mathbf{U}$; $\mathbf{R}_1^u = \mathbf{Q}_1^u + \tau_1\,\mathbf{U}$ (40)

Regarding Equations (36) and (40), the points $[\mathbf{P}_x,\mathbf{Q}_x,\mathbf{R}_x]$ are successively in a line, and the tangent vectors $[\mathbf{P}_0^u,\mathbf{Q}_0^u,\mathbf{R}_0^u]$, and $[\mathbf{P}_1^u, \mathbf{Q}_1^u,\mathbf{R}_1^u]$ are successively in the same tangent planes $[\mathbf{Q}_0^u,\mathbf{U}]$ and $[\mathbf{Q}_1^u,\mathbf{U}]$. Then, for every value u in the interval $0 \le u \le 1$, the generatrix lines $[\mathbf{Q}(u)\text{-}\mathbf{P}(u)]$ and $[\mathbf{R}(u)\text{-}\mathbf{P}(u)]$ coincide and parallel to the vector $\mathbf{U}$. Therefore, the generalized cylinder surface that is bounded by the Hermite curves $[\mathbf{P}(u),\mathbf{R}(u)]$ is as follows:

$$\begin{aligned}\mathbf{D}(u,v) &= (1\text{-}v)\,\mathbf{P}(u) + v\,\mathbf{R}(u)\\ &= (1\text{-}v)\,\{F_1(u)\,(\mathbf{Q}_0 - \alpha_0\mathbf{U}) + F_2(u)\,(\mathbf{Q}_{1/3} - \alpha_{1/3}\mathbf{U}) + F_3(u)\,(\mathbf{Q}_{2/3} - \alpha_{2/3}\mathbf{U}) + F_4(u)\,(\mathbf{Q}_1 - \alpha_1\mathbf{U}) +\\ &\quad F_5(u)\,(\mathbf{Q}_0^u - \rho_0\,\mathbf{U}) + F_6(u)\,(\mathbf{Q}_1^u - \rho_1\,\mathbf{U})\} +\\ &\quad v\,\{F_1(u)\,(\mathbf{Q}_0 + \beta_0\mathbf{U}) + F_2(u)\,(\mathbf{Q}_{1/3} + \beta_{1/3}\mathbf{U}) + F_3(u)\,(\mathbf{Q}_{2/3} + \beta_{2/3}\mathbf{U}) + F_4(u)\,(\mathbf{Q}_1 + \beta_1\mathbf{U}) +\\ &\quad F_5(u)\,(\mathbf{Q}_0^u + \tau_0\,\mathbf{U}) + F_6(u)\,(\mathbf{Q}_1^u + \tau_1\,\mathbf{U})\}\end{aligned} \quad (41)$$

where, $\alpha_0, \alpha_{1/3}, \alpha_{2/3}, \alpha_1, \rho_0, \rho_1 > 0$; $\beta_0, \beta_{1/3}, \beta_{2/3}, \beta_1, \tau_0, \tau_1 > 0$; and $0 \le u,v \le 1$.

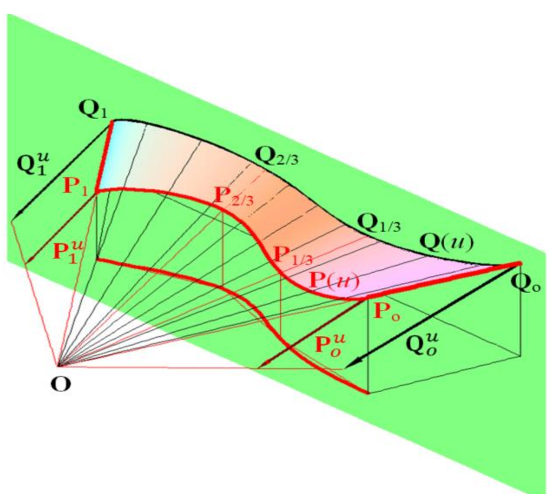

Figure 7. Calculated control points and tangent vectors of the Hermite curve $\mathbf{P}(u)$.

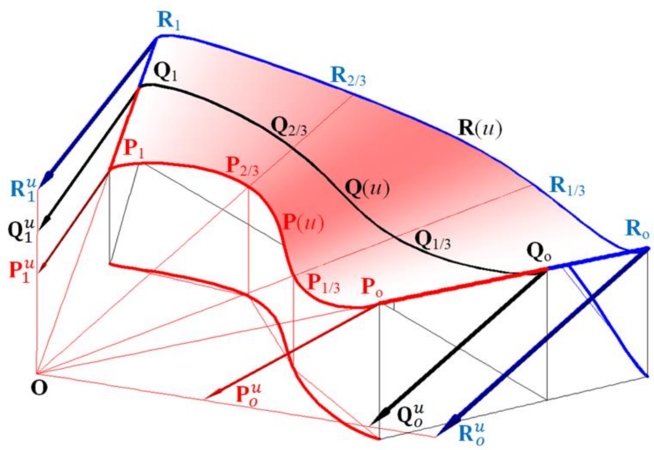

Figure 8. Quintic developable Hermite surface.

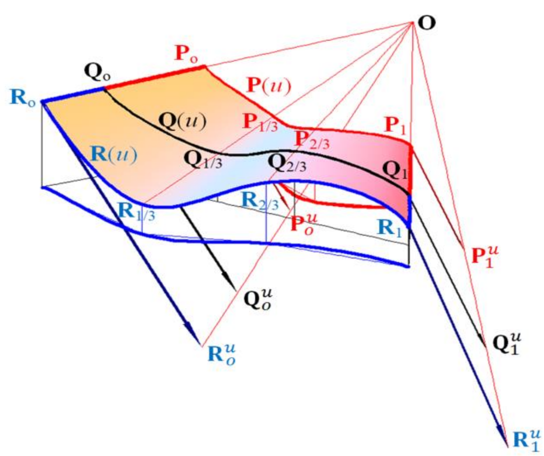

Figure 9. Position of the tangent vectors [$\mathbf{P}_0^u$,$\mathbf{P}_1^u$] and [$\mathbf{R}_0^u$,$\mathbf{R}_1^u$].

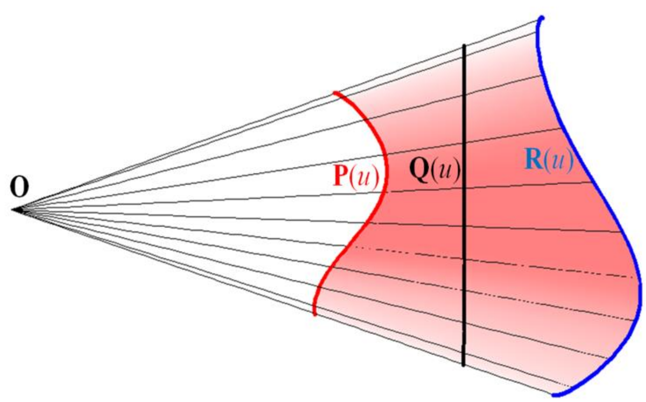

Figure 10. Boundary curves profile of the quintic developable Hermite surface.

The calculation for constructing the cylinder surface laid between the quintic Hermite curves [$\mathbf{P}(u)$,$\mathbf{R}(u)$] consists of some steps: (a) determine the control points' data [$\mathbf{Q}_o$,$\mathbf{Q}_{1/3}$,$\mathbf{Q}_{2/3}$,$\mathbf{Q}_1$] and two tangent vectors [$\mathbf{Q}_0^u$,$\mathbf{Q}_1^u$] in the plane $\mathbf{\Psi}$, and the fixed nonzero direction vector $\mathbf{U}$ unparallel to this plane $\mathbf{\Psi}$ (Figure 11); (b) Apply Equations (36) and (40) to compute the control points respectively [$\mathbf{P}_o$,$\mathbf{P}_{1/3}$,$\mathbf{P}_{2/3}$,$\mathbf{P}_1$], [$\mathbf{R}_o$,$\mathbf{R}_{1/3}$,$\mathbf{R}_{2/3}$,$\mathbf{R}_1$], and the tangent vectors [$\mathbf{P}_0^u$,$\mathbf{P}_1^u$], [$\mathbf{R}_0^u$,$\mathbf{R}_1^u$]; and (c) plot the quintic developable Hermite surface $\mathbf{D}(u,v)$ by using Equation (41).

***Simulation* 6**

Arranging data $\mathbf{Q}_0$ = <-20,60,30>, $\mathbf{Q}_{1/3}$ = <-20,30,40>, $\mathbf{Q}_{2/3}$ = <-20,-25,20>, $\mathbf{Q}_1$ = <-20,-60,25>, $\mathbf{Q}_0^u$ = <0,-40,60>, $\mathbf{Q}_1^u$ = <0,-40,60>, $\mathbf{U}$ = <-2/√6, 1/√6, 1/√6>, α_0 =20, $\alpha_{1/3}$ =40, $\alpha_{2/3}$ =30, α_3 =45, ρ_0 =10, ρ_1 =10, and implementing Equation (36) obtain the control points $\mathbf{P}_0$ = <-3.7,51.8,21.8>, $\mathbf{P}_{1/3}$ = <12.6,13.6,23.6>, $\mathbf{P}_{2/3}$ = <4.5,-37.3,7.7>, $\mathbf{P}_1$ = <16.7,-78.4,6.6>, and the tangent vectors $\mathbf{P}_0^u$ = <8.2,-44.1,55.9>, $\mathbf{P}_1^u$ = <8.2,-44.1,55.9> as shown in Figure 11. Furthermore, given β_0 = 15, $\beta_{1/3}$ = 30, $\beta_{2/3}$ = 30, β_1 = 25, τ_0 = 10, τ_1 = 10. Computing Equation (40), we obtain $\mathbf{R}_0$ = <-32.2,66.1,36.1>, $\mathbf{R}_{1/3}$ = <-44.5,42.3,52.3>, $\mathbf{R}_{2/3}$ = <-44.5,-12.7,32.3>, $\mathbf{R}_1$ = <-40.4,-49.8,35.2>, and the tangent vectors $\mathbf{R}_0^u$ = <-8.2,-35.9,64.1>, $\mathbf{R}_1^u$ = <-8.3,-35.9,64.1>. From these calculation data, using Equation (41) can construct the quintic developable Hermite surfaces limited with the space curves [$\mathbf{P}(u)$,$\mathbf{R}(u)$] in Figure 12.

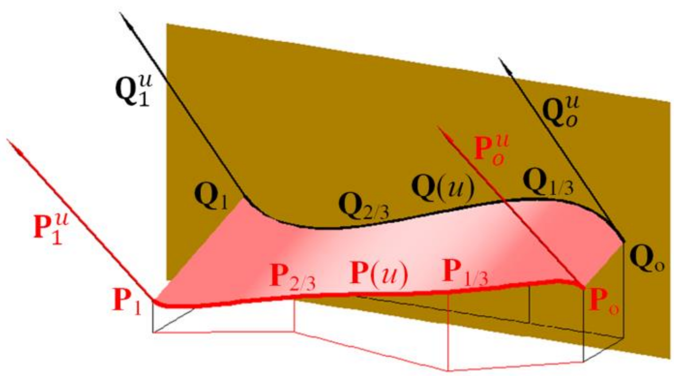

Figure 11. Calculated control points [$\mathbf{P}_0$, $\mathbf{P}_1$, $\mathbf{P}_2$, $\mathbf{P}_3$, $\mathbf{P}_4$, $\mathbf{P}_5$] of Hermite cylinder surface.

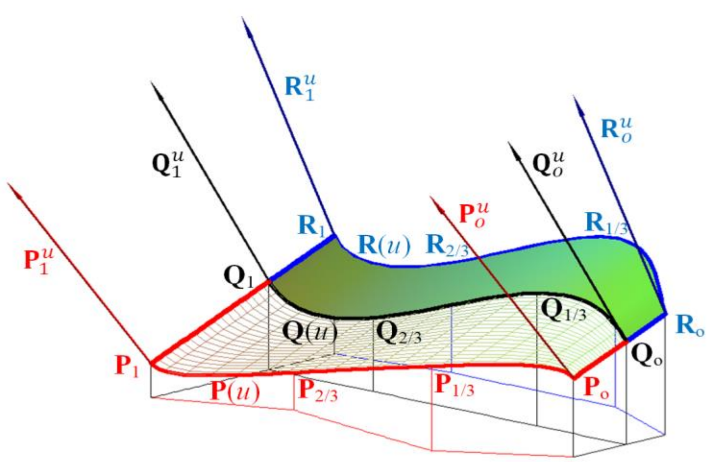

Figure 12. Designing Hermite cylinder surface with the boundary curves [$\mathbf{P}(u)$, $\mathbf{R}(u)$].

In general, the presented method offers to design the developable surface with various arches shapes (Figure 8 and Figure 12). We can easily pose the control points [$\mathbf{Q}_o$,$\mathbf{Q}_{1/3}$,$\mathbf{Q}_{2/3}$,$\mathbf{Q}_1$] and the tangent vectors [$\mathbf{Q}_0^u$,$\mathbf{Q}_1^u$] for changing curve $\mathbf{Q}(u)$ arches to create the developable surface models of the cone and cylinder type. Arranging the data respectively [σ_0, $\sigma_{1/3}$, $\sigma_{2/3}$, σ_1, ρ_0, ρ_1], [δ_0, $\delta_{1/3}$, $\delta_{2/3}$, δ_1, τ_0, τ_1], and [α_0, $\alpha_{1/3}$, $\alpha_{2/3}$, α_1, ρ_0, ρ_1], [β_0 , $\beta_{1/3}$, $\beta_{2/3}$, β_1, τ_0, τ_1] for both Equations (32) and (41) can effectively design and modify the desired profile of both boundary curves [$\mathbf{P}(u)$,$\mathbf{R}(u)$] of the developable surface types.

4. Conclusion

We have introduced the algebraic equations and the numerical procedure to design the developable surfaces bounded by the space curves in two following ways. First, by using control points and tangent vectors of quintic Bézier/Hermite curves in a plane, a fixed point outside the plane, and second, by utilizing the criteria equations to arrange the control points' position in space, we can formulate two equations of Bézier/Hermite curves situated in the different side of this plane. Substituting these curve equations to the surface equations of two curves interpolation finds the developable surfaces of cone type. Second, by passing control points and tangents vectors of quintic Bézier/Hermite curves in a plane, a fixed non-zero constant vector unparallel to the plane, and employing the criteria equations to determine the control points' position in space, we can formulate the two equations of Bézier/Hermite curves laid in the different side of the plane. Inserting these curve equations into the surface equations of two curves by interpolation, obtains the developable surfaces of cylinder type.

Comparing the presented method of this research with previous studies shows that the proposed method provides some benefits for modeling developable surfaces. Arranging the control points of the Bézier/Hermite curve in the plane gives a chance to modify the developable surface shapes and their fluctuations. Also, the surface arches change to be up or down more than twice. We can effectively use the fixed parameters in these surface equations of two curves interpolation to change and adjust the desired profile of both boundary curves of the developable surfaces. In this case, giving different parameter values to these equations modifies the arch shapes of the boundary curves in two directions of the generatrix lines of the surfaces. From these benefits, the results are applicable to design the metal and plywood sheets installation for skinning great industrial objects.

Modeling developable surfaces from the control points and the tangent vector data of a curve in the plane have been presented. In further studies, the interesting thing is to model the developable surfaces using these control points and the tangent vector data in space.

Conflicts of Interest

The authors confirm that there is no conflict of interest to declare for this publication.

Acknowledgments

The author wants to acknowledge the editor and anonymous reviewers for their comments and suggested improvements.

References

Abbena, E., Salamon, S., & Gray, A. (2006). *Modern differential geometry of curves and surfaces with Mathematica*. Chapman & Hall/CRC, London.

Abdel-Baky, R.A., & Unluturk, Y. (2020a). The relatively osculating developable surfaces of a surface along a direction curve. *Communications Faculty of Sciences University of Ankara-Series A1 Mathematics and Statistics*, *69*(1), 511-527. https://doi.org/10.31801/cfsuasmas.527231.

Abdel-Baky, R.A., & Unluturk, Y. (2020b). Normal developable surfaces of a surface along a direction curve. *Journal of the Indonesian Mathematical Society*, *26*(3), 319-333. https://doi.org/10.22342/jims.26.3.872.319-333.

Al-Ghefari, R.A., & Abdel-Baky, R.A. (2013). An approach for designing developable surface with a common geodesic curve. *International Journal of Contemporary Mathematical Sciences*, *8*, 875-891.

Ammad, M., Misro, M.Y., Abbas, M., & Majeed, A. (2021). Generalized developable cubic trigonometric Bézier surfaces. *Mathematics*, *9*(3), 283. https://doi.org/10.3390/math9030283.

Fernández-Jambrina, L., & Pérez-Arribas, F. (2020). Developable surface patches bounded by NURBS curves. *Journal of Computational Mathematics*, *38*, 715-731. https://doi.org/10.4208/jcm.1904-m2018-0209.

Frey, W.H., & Bindschadler, D. (1993). *Computer-aided design of a class of developable Bézier surfaces*. General Motors R&D Publication, Detroit.

Hu, G., Wu, J., & Qin X. (2018). A new approach in designing of local controlled developable HBézier surfaces. *Advances Engineering Software*, *121*, 26-38. http://dx.doi.org/10.1016/j.advengsoft.2018.03.003.

Julius, D.N. (2006). *Developable surface processing methods for 3D meshes* [Master thesis, University of British Columbia]. UBC Library. https://webcat.library.ubc.ca/vwebv/holdingsInfo?bibId=3742697.

Kusno (2019). Construction of regular developable Bézier patches. *Mathematical and Computational Applications*, *24*(4), 1-13. https://doi.org/10.3390/mca24010004.

Kusno (2020a). Modeling of developable surfaces using Hermite spline interpolation curves. *Advances in Mathematics: Scientific Journal*, *9*(10), 8431-8442. https://doi.org/10.37418/amsj.9.10.72.

Kusno (2020b). Fitting a curve, cutting surface, and adjusting the shapes of developable Hermite patches. *Mathematics and Statistics*, *8*(6), 740-746. https://doi.org/10.13189/ms.2020.080615.

Kusno (2021). On the modeling of developable Hermite patches. *Journal of Mathematical and Computational Science*, *11*(2), 1145-1165. https://doi.org/10.28919/jmcs/5293.

Li, C., & Zhu, C. (2020). Designing developable C-Bézier surface with shape parameters. *Mathematics*, *8*(3), 1-21. .https://doi.org/10.3390/math8030402.

Lipschutz, M. (1969). *Theory and problems of differential geometry (Schaum's outline series)*. McGraw-Hill, New York.

Mortenson, M.E. (1986). *Geometric modeling*. John Wiley & Sons, New York.

Park, F.C., Yu, Y., Chun, C., & Ravani, B. (2002). Design of developable surfaces using optimal control. *Journal of Mechanical Design*, *124*(4), 602-608. https://doi.org/10.1115/1.1515795.

Xu, G., Li, M., Mourrain, B., Rabczuk, T., Xu, J., & Bordas, S. (2017). Constructing IGA-suitable planar parameterization from complex CAD boundary by domain partition and global/local optimization. *Computer Methods in Applied Mechanics and Engineering*, *328*, 175-200. http://dx.doi.org/10.1016/j.cma.2017.08.052.

Yu, X. (2017). *Math 348 differential geometry of curves and surfaces (Lecture 10 applications of the first fundamental form)*. Department of Mathematical & Statistical Sciences, University of Alberta. http://www.math.ualberta.ca/~xinweiyu/348.A1.17f/L10_FFF_II_20171012_Slides.pdf.

Zhao, H., & Wang, G. (2008). A new method for designing a developable surface utilizing the surface pencil through a given curve. *Progress in Natural Science*, *18*(1), 105-110. https://doi.org/10.1016/j.pnsc.2007.09.001.

Original content of this work is copyright © International Journal of Mathematical, Engineering and Management Sciences. Uses under the Creative Commons Attribution 4.0 International (CC BY 4.0) license at https://creativecommons.org/licenses/by/4.0/

Publisher's Note- Ram Arti Publishers remains neutral regarding jurisdictional claims in published maps and institutional affiliations.